

Regularly Distributed and Fully Accessible Pt Nanoparticles in Silica Pore Channels via the Controlled Growth of a Mesoporous Matrix around Pt Colloids

Malika Boualleg,[†] Jean-Marie Basset,[†]
Jean-Pierre Candy,[†] Pierre Delichere,[‡] Katrin Pelzer,[§]
Laurent Veyre,[†] and Chloé Thieuleux^{*,†}

Université de Lyon, Institut de Chimie de Lyon, UMR 5265
CNRS-Université de Lyon-ESCE Lyon, LC2P2, Equipe Chimie
Organométallique de Surface, ESCPE 43 Boulevard du 11
Novembre 1918, F-69616 Villeurbanne, France, Université de
Lyon, Institut de Chimie de Lyon, UMR 5256 CNRS-Université
de Lyon 1, IRCE Lyon, 2 avenue A. Einstein F-69616
Villeurbanne, France, and Fritz-Haber-Institute of the Max
Planck Society, Faradayweg 4-6, 14195 Berlin, Germany

Received November 7, 2008

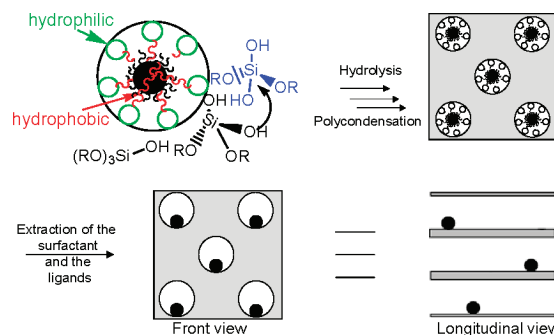
Revised Manuscript Received January 13, 2009

Since the discovery of the first mesoporous oxides in the early 1990s,^{1,2} scientists have focused on developing synthetic procedures to fine-tune the pore network structure and pore size distribution of various materials.^{1,3} These fine-tuned porous materials found applications as absorbers, catalysts, or catalyst supports and more recently in separation, medical diagnosis, or microelectronics.⁴

So far, many attempts to include metal particles in mesoporous oxides were performed. Inter alia one may mention (i) metal ion exchange reactions and in situ reduction of the metal,⁵ (ii) chemical vapor deposition of metal compounds and their subsequent decomposition,⁶ and (iii) incipient wetness or impregnation.⁷ These classical techniques led to the successful incorporation of particles of several metals onto porous supports but they did not provide a sufficient control over the metal particle size or the particle distribution in the material. This lack of control could be responsible for the reduced catalyst productivity and the premature particle sintering.

Recently, self-assembly pathways to generate arrays of supported nanoparticles⁸ have shown very attractive results and thus, the controlled growth by sol–gel process of a hierarchically organized silica matrix around a colloidal solution of metal nanoparticles using supramolecular interactions between a surfactant (used as the structure directing agents of the oxide matrix) and metal colloids could be an attractive way to overcome the aforementioned problems faced with classical synthetic procedures. In this field, two pioneer reports^{9,10} have established the validity of the concept of such an approach (Scheme 1). Nevertheless, improvements in the synthetic procedures are necessary either to overcome the incomplete metal incorporation⁹ or to circumvent the presence of tricky stabilizing ligands¹⁰ such as polyvinylpyrrolidone (PVP), which are difficult to remove from the metal particles without their sintering and which is not compatible with acidic media generally used for obtaining highly structured silica matrixes.¹¹

Scheme 1. Principle Underlying the Synthesis of a Highly Structured Silica Containing Regularly Distributed Pt Particles along Its Channel Pores Knowing That the Nanoparticles Should Enter the Hydrophobic Core of the Surfactant Micelles without Destroying the Surfactant Mesophase



Thus, we describe herein a simple procedure to prepare a highly structured silica containing regularly distributed Pt particles along its channel pores, such nanoparticles being incorporated in a quantitative yield. These materials were obtained by the controlled growth of a mesoporous silica matrix around a colloidal solution of Pt nanoparticles using the *n*-octylsilane as the stabilizing ligand.

This controlled growth was achieved working around a fundamental requirement: the nanoparticles would have to enter the hydrophobic core of the surfactant micelles without destroying the surfactant mesophase (scheme 1). Several parameters were thus secured: (i) a strong non-exchangeable stabilizing

* Corresponding author. E-mail: thieuleux@cpe.fr.

[†] LC2P2, Equipe COMS, ESCPE Lyon.

[‡] IRCE Lyon, Université de Lyon 1.

[§] Fritz-Haber-Institute of the Max Planck Society.

- (1) Kresge, C. T.; Leonowicz, M. E.; Roth, W. J.; Vartuli, J. C.; Beck, J. S. *Nature* **1992**, *359*, 710.
- (2) Beck, J. S.; Vartuli, J. C.; Roth, W. J.; Leonowicz, M. E.; Kresge, C. T.; Schmitt, K. D.; Chu, T. W.; Olson, D. H.; Sheppard, E. W.; McCullen, S. B.; Higgins, J. B.; Schlenker, J. L. *J. Am. Chem. Soc.* **1992**, *114*, 10834.
- (3) (a) Bagshaw, S. A.; Prouzet, E. T.; Pinnavaia, J. *Science* **1995**, *269*, 1242. (b) Tanev, P. T.; Pinnavaia, T. J. *Science* **1995**, *267*, 865. (c) Huo, Q. S.; Margolese, D. I.; Ciesla, U.; Feng, P. Y.; Gier, T. E.; Sieger, P.; Leon, R.; Petroff, P. M.; Schuth, F.; Stucky, G. D. *Nature* **1994**, *368*, 317. (d) Zhao, D.; Huo, Q.; Feng, J.; Chmelka, B. F.; Stucky, G. D. *J. Am. Chem. Soc.* **1998**, *120*, 6024. (e) Zhao, D.; Feng, J.; Huo, Q.; Melosh, N.; Frederickson, G. H.; Chmelka, B. F.; Stucky, G. D. *Science* **1998**, *279*, 548. (f) Matos, J. R.; Kruk, M.; Mercuri, L. P.; Jaroniec, M.; Zhao, L.; Kamiyama, T.; Terasaki, O.; Pinnavaia, T. J.; Liu, Y. J. *J. Am. Chem. Soc.* **2003**, *125*, 821.
- (4) Davis, M. E. *Nature* **2002**, *417*, 813.
- (5) (a) Goguet, A.; Schweich, D.; Candy, J. P. *J. Catal.* **2003**, *220*, 280. (b) Chytil, S.; Glomm, W. R.; Kvande, I.; Zhao, T.; Walmsley, J. C.; Blekkan, E. A. *Top. Catal.* **2007**, *45*, 93.
- (6) Benesis, A. H.; Curtis, R. M.; Studer, H. P. *J. Catal.* **1968**, *10*, 328.
- (7) Konya, Z.; Molnar, E.; Tasi, G.; Niesz, K.; Somorjai, G. A.; Kiricsi, I. *Catal. Lett.* **2007**, *113*, 19.

- (8) (a) Wright, A.; Gabaldon, J.; Burckel, D. B.; Jiang, Y. B.; Tian, Z. R.; Liu, J.; Brinker, C. J.; Fan, H. Y. *Chem. Mater.* **2005**, *18*, 3034. (b) Fan, H. Y.; Yang, K.; Boye, D.; Sigmon, T.; Malloy, K.; Xu, H.; Lopez, G. P.; Brinker, C. *Science* **2004**, *304* (5670), 567.
- (9) Aprile, C.; Abad, A.; Garcia, H.; Corma, A. *J. Mater. Chem.* **2005**, *15*, 4408.
- (10) Song, H.; Rioux, R. M.; Hoefelmeyer, J. D.; Komor, R.; Niesz, K.; Grass, M.; Yang, P.; Somorjai, G. A. *J. Am. Chem. Soc.* **2006**, *128*, 3027.
- (11) (a) Huo, Q.; Margolese, D. I.; Ciesla, U.; Feng, P.; Gier, T. E.; Sieger, P.; Leon, R.; Petroff, P. M.; Schuth, F.; Stucky, G. D. *Nature* **1994**, *368*, 317. (b) Huo, Q.; Margolese, D. I.; Stucky, G. D. *Chem. Mater.* **1996**, *8*, 1147.

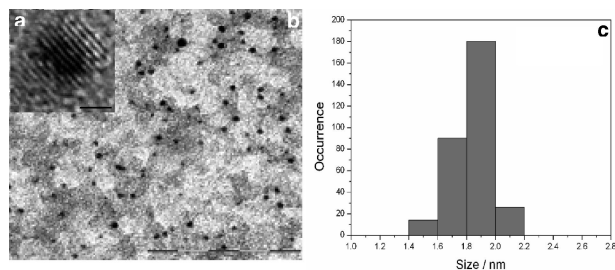


Figure 1. (a, b) TEM micrographs of the Pt nanoparticles solution (bar scales: $a = 1$ nm, $b = 50$ nm), (c) size histogram of Pt nanoparticles (calculated using ~ 200 particles).

ligand in order to avoid exchanges with the surfactant or the evolved alcohol during the sol–gel process, (ii) at the same time, a highly hydrophobic one, in order to enter the micelles; *n*-octylsilane was chosen and (iii) an overall compatibility between the size of the micelles (and thus ultimately the material pores), and the diameter of the stabilized nanoparticles (and thus ultimately the NPs in the pores). We thus adjusted the nanoparticles size, the pH, the type and size of the surfactant and the condensation catalyst in order to address this parameter.

Following a typical procedure developed for the synthesis of Ru particles stabilized by silane ligands,¹² we successfully prepared sufficiently small crystalline Pt nanoparticles by contacting $\text{Pt}(\text{dba})_2$ with 0.5 equiv. of *n*-octylsilane in THF as solvent. After several hours at room temperature under 3 bar of dihydrogen, a black suspension of nanoparticles was obtained as a solution containing monodispersed nanoparticles whose size are measured at 2 ± 0.4 nm by transmission electron microscopy and calculated with an histogram of ca. 200 particles (Figure 1). Elemental analyses, IR experiments, and XPS measurements confirmed the presence of silane ligands at the surface of the particles¹³ (see Figures S1 and S2 in the Supporting Information). A total of 0.38 equiv of Si atoms per Pt atoms was found and corroborated the fact that 0.3–0.4 equiv. of ligands is sufficient to fully cover the surface particles.

Second, we undertook the synthesis of the material by reaction of the aforementioned solution (12 mL, 17.9 μmol) with an acidic aqueous solution of Pluronic P123 surfactant (1.7 g of P123 in 63 mL of deionized water, pH 1.5) and TEOS (3.53 g, 17 mmol) as the precursor of the oxide matrix. After the slow evacuation of the THF, the resulting suspension was stirred for 3 h prior to heating at 318 K and NaF (30 mg) was added. After 48 h of aging, the resulting deep gray precipitate was filtered off, washed and finally dried under vacuum (10^{-5} mBar) at 400 K overnight.

The elemental analyses of this as-synthesized solid showed the quantitative incorporation of the Pt nanoparticles (found: 0.30 ± 0.05 wt %, expected: 0.35 ± 0.05 wt %). Small-angle X-ray diffraction displayed the signals corresponding to a 2D hexagonal long-range ordering of the channel pores (see Figure S3 in the Supporting Information). The transmission electron microscopy confirmed this order (images a and b in Figure 2) and also showed (i) the random distribution of the particles in the silica matrix (no agglomeration of particles was observed,

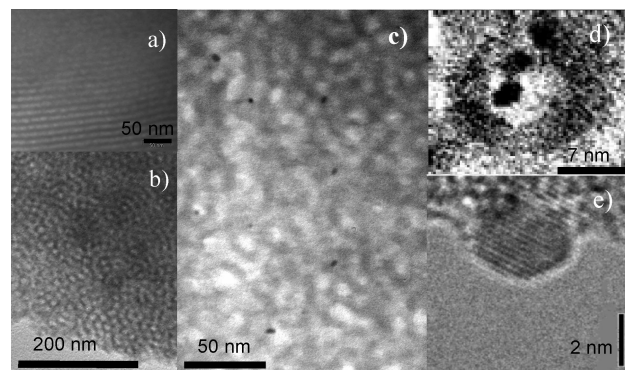


Figure 2. TEM micrographs of the as-synthesized Pt containing nanostructured material (bar scales: $a = 50$ nm, $b = 200$ nm, $c = 50$ nm, $d = 7$ nm, $e = 2$ nm).

see Figure 2c), (ii) the location of such particles at the surface of the pores (Figure 2d), and (iii) the size of the particles (2.2 ± 0.2 nm) as well as the crystallographic arrangements of the Pt lattice fringes (0.26 Å) of the particles (Figure 2e). The size of the crystallites (2.3 ± 0.5 nm) was also measured by wide angle X-ray diffraction analyses using the Scherrer model (see Figure S4 in the Supporting Information).

In summary, the as-synthesized material showed the successful incorporation of Pt nanoparticles while retaining superior material mesostructure.

The removal of the surfactant and the aliphatic chain of the stabilizing ligands from the as-synthesized material were achieved by calcination under dry air at 593 K, and this method proved to be the best adapted with respect to calcination at higher temperature (723 K), thermolysis (treatment under dry Argon at 723 K), hydrogenolysis (treatment under dry hydrogen at 723 K), and extraction at the reflux of ethanol in a Soxhlet apparatus since it ensured no disruption in the material structuration and a limited sintering of the nanoparticles according to electron microscopy, wide-angle X-Ray diffraction and N_2 adsorption (see Figures S5 and S7–S9 in the Supporting Information). The aforementioned techniques also clearly indicated that (i) calcination or hydrogenolysis at very high temperature (ca. 773 K) led to the complete removal of the surfactant but unfortunately to the total sintering of the particles within the material (Table 1, entries 2 and 4, and Figures S14–S17 in the Supporting Information) (ii) thermolysis, even at high temperature did not ensure the quantitative removal of the surfactant as shown by the black aspect of the solid and the important decrease of the surface area (Table 1, entry 3) and led to the partial sintering of the particles (see Figures S11–S13 in the Supporting Information), and (iii) the Soxhlet extraction induced the partial lixiviation of the particles and their subsequent agglomeration within the material (see Figures S18–S20 in the Supporting Information).

For comparison, a catalyst was prepared by loading a mesostructured silica matrix with Pt particles by a colloidal impregnation and further treated under calcination at 593 K. The TEM micrographs of the resulting solid showed the complete sintering of the metal particles in the silica matrix (Figure 3b) as confirmed by the absence of catalytic activity for the solid. This observations thus suggested a lack of control in the metal particles distribution when impregnation techniques are used and highlighted the uniform distribution of the Pt

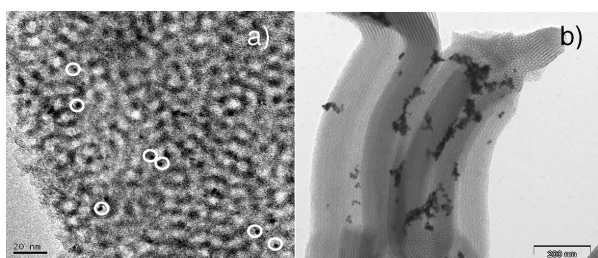
(12) (a) Pelzer, K.; Laleu, B.; Lefebvre, F.; Philippot, K.; Chaudret, B.; Candy, J.-P.; Basset, J.-M. *Chem. Mater.* **2004**, *16*, 4937. (b) Pelzer, K.; Candy, J.-P.; Bergeret, G.; Basset, J.-M. *Eur. Phys. J. D.* **2007**, *43*, 197.

(13) Chechal, J.; Sikola, T. *Surf. Sci.* **2006**, *600*, 4717.

Table 1. Characteristics of the Pt-Containing Mesostructured Materials before and after Removal of the Surfactant using the Different Treatments

entry	treatment	V_p (cm ³ /g)	D_p^a (nm)	S_{BET} (m ² /g)	$d_{particle}^b$ (nm)
1	calcination (773 K)	1.5	7.5	1100	>7
2	calcination (593 K)	1.5	8	1100	3.5
3	thermolysis (700 K)	0.7	8.5	540	4.5
4	hydrogenolysis (723 K)	1.0	7.5	875	7
5	Soxhlet extraction	1.3	7.5	820	3

^a Porous diameter obtained using BJH model at the adsorption branch of the isotherm. ^b Mean diameter of the Pt particles given by wide-angle X-Ray diffraction.

**Figure 3.** TEM micrographs of (a) the calcinated Pt containing material and (b) the Pt impregnated SBA-15 (bar scales = 20 and 200 nm).

particles within the material when a controlled growth of silica matrix around metal colloids was performed.

Upon calcination, the surfactant was completely removed as shown by N₂ adsorption/desorption measurements which provided an isotherm of type IV, characteristic of mesoporous material (see Figure S9 in the Supporting Information). The calcinated material displayed a high surface area of 1100 m²/g, a pore volume of 1.5 cm³/g, and a narrow pore size distribution at 8 nm (strictly corresponding to the expected characteristic for a pure mesoporous silica prepared in the same conditions). This treatment did not change the Pt loading (0.3 wt % given by elemental analysis) and slightly increased the mean size of the Pt nanoparticles from 2.5 to 3.5 nm as measured by wide-angle X-ray diffraction using the Scherrer model and TEM micrographs (Figure 3a) (measured size = 3.5 nm corresponding to a dispersion of 34%; see Figures S6 and S7 in the Supporting Information), whereas H₂ and O₂ chemisorption methods yielded particles size of 4.1 nm (Pt dispersion of 31%, see Table S1 in the Supporting Information). Noteworthy, the presence of Si atoms on the surface of the particles and the absence of platinum oxide, even after calcination, were observed by XPS analysis, which provided a spectrum comparable to that of the initial colloidal solution (see Figure S8 and Table S2 in the Supporting Information). These Si atoms can contribute to the slight decrease of the observed H₂ and O₂ chemisorption on the particles compared to XPS measurements.

The catalytic performances of the mesostructured Pt containing material were studied using the propene hydrogenation¹⁴

and compared to that of (i) a classical and commercially available heterogeneous catalyst (Pt/Al₂O₃) obtained by metal salts decomposition and to (ii) the aforementioned impregnated SBA-15 silica after calcination at 593 K. Because of its similarity with our material in term of metal loading and metal dispersion (0.32 wt % and a metal dispersion of 70–80%), the commercially available reference catalyst (Pt/Al₂O₃) was chosen even if the support was alumina and not silica. However, this catalytic reaction did not seem to be support dependent¹⁵ and thus, this change from SiO₂ to Al₂O₃ should not influence drastically the catalytic results. The propene hydrogenation reaction was performed at 278 K in a continuous flow reactor using 7 mg of catalyst and a constant flow of H₂/He/propene (20/16/1.09 cm³/min). The catalytic performances of the impregnated SBA-15 were found to be extremely low (TOF < 0.02 s⁻¹) compared to that of our catalyst, thus showing the real benefit of the regular distribution of the nanoparticles compared to that of a colloidal impregnation route. The activity of the Pt containing mesostructured material was also very similar to that of the reference sample Pt/Al₂O₃ in term of turn over frequency: the TOF is about 0.9 s⁻¹ per surface Pt atom for both catalysts (see Figure S10 in the Supporting Information). These catalytic performances were in good agreement with the estimated size of the nanoparticles (given by TEM and XRD) and more surprisingly, it highlighted the fact that the presence of Si atoms on the surface of particles does not seem to be detrimental for the accessibility or for the reactivity of the Pt nanoparticles in catalysis.

In summary, we have prepared and characterized a highly structured material containing regularly distributed Pt nanoparticles via the controlled growth of a mesostructured silica matrix around Pt colloids.

Using optimized thermal treatments, the materials were fully characterized using several analytical techniques and it was shown that (i) the Pt nanoparticles are still quantitatively present and regularly distributed along the channel pores of the material, (ii) very little sintering is observed, and (iii) the stabilizing ligand bonded to the Pt nanoparticles is successfully removed, thus leading to a highly active Pt containing nanostructured catalyst for the propene hydrogenation reaction.

It is noteworthy that this methodology can be broadened to other types of metal particles, thus providing original, robust, and stable mesostructured NPs containing materials of great interest for the field of heterogeneous catalysis.

Acknowledgment. We thank Dr G. Bergeret for the WAXS experiments and the “Centre Technologique des Microstructures” for TEM micrographs.

Supporting Information Available: Characterization of the Pt colloids and materials (PDF). This material is available free of charge via the Internet at <http://pubs.acs.org>.

CM803031C

(14) Oterschipper, P. H.; Wachter, W. A.; Butt, J. B.; Burwell, R. L.; Cohen, J. B. *J. Catal.* **1977**, *50*, 494.

(15) Cocco, G.; Campostrini, R.; Cabras, M. A.; Carturan, G. *J. Mol. Catal.* **1994**, *94*, 299.